Unscreened Hartree-Fock calculations for metallic Fe, Co, Ni, and Cu from *ab initio* Hamiltonians

I. Schnell,[1,2] G. Czycholl,[2] and R. C. Albers[1]
[1]*Theoretical Division, Los Alamos National Laboratory, Los Alamos, New Mexico 87545, USA*
[2]*Department of Physics, University of Bremen, P.O. Box 330 440, D-28334 Bremen, Germany*
(Received 16 April 2003; revised manuscript received 23 July 2003; published 2 December 2003)

Unscreened Hartree-Fock approximation (HFA) calculations for metallic Fe, Co, Ni, and Cu are presented, by using a quantum-chemical approach. To the best of our knowledge these are the first HFA results to have been done for crystalline 3*d* transition metals. Our approach uses a linearized muffin-tin orbital calculation to determine Bloch functions for the Hartree one-particle Hamiltonian, and from these obtains maximally localized Wannier functions, using a method proposed by Marzari and Vanderbilt. Within this Wannier basis all relevant one-particle and two-particle Coulomb matrix elements are calculated. The resulting second-quantized multiband Hamiltonian with *ab initio* parameters is studied within the simplest many-body approximation, namely the unscreened, self-consistent HFA, which takes into account exact exchange and is free of self-interactions. Although the *d* bands sit considerably lower within HFA than within the local (spin) density approximation LSDA, the exchange splitting and magnetic moments for ferromagnetic Fe, Co, and Ni are only slightly larger in HFA than what is obtained either experimentally or within LSDA. The HFA total energies are lower than the corresponding LSDA calculations. We believe that this same approach can be easily extended to include more sophisticated *ab initio* many-body treatments of the electronic structure of solids.

DOI: 10.1103/PhysRevB.68.245102 PACS number(s): 71.10.Fd, 71.15.Ap, 71.15.Mb, 71.20.Be

I. INTRODUCTION

In this paper we use a quantum-chemical approach to present unscreened Hartree-Fock approximation (HFA) calculations of metallic Fe, Co, Ni, and Cu. Because our approach uses localized Wannier functions, it is a Hubbard-like method that should be easily generalized to include more sophisticated many-body treatments of correlation effects. Nonetheless, it is useful to understand what a HFA method would give before moving on to consider correlation. To place these calculations in context it is useful to briefly review the status of electronic-structure calculations in solids.

Most existing *ab initio* (first-principles) methods for the numerical calculation of the electronic properties of solids are based on density-functional theory (DFT),[1] which in principle is exact and properly takes into account many-body effects involving the Coulomb interaction between the electrons; for an overview on the present status of DFT we refer to the books in Refs. 2 and 3. But, in general, the functional dependence of the kinetic energy and the exchange and correlation part of the Coulomb (interaction) energy on the electron density are not known explicitly, and hence additional approximations and assumptions are necessary. A well-established additional approximation is the local-density approximation (LDA)[4] (or local spin-density approximation LSDA for magnetic systems), which assumes that the exchange-correlation potential depends locally on the electronic density. Even then, the functional dependence of the exchange-correlation energy on the density is not known in general, and it is usually necessary to make an ansatz for the exchange-correlation functional, which is based on the homogeneous electron gas. The LDA goes beyond the simplest electron-gas approximation, the HFA, in that correlation energy is explicitly taken into account. On the other hand, the HFA exchange potential is nonlocal, i.e., the potential at point $\mathbf{r}$ depends on the density at all other positions $\mathbf{r}'$, an effect which the LDA exchange potential misses. However, in practice LDA treatments are simpler than HFA calculations, because local exchange is easier to treat than nonlocal exchange, and are usually in better agreement with experiment. Therefore, DFT (LDA-like) treatments have been far more common than HFA during the past few decades, even in quantum chemistry (with a long tradition of methods based on HFA).

Ab initio DFT-LDA calculations have been very successful for many materials and ground-state properties such as crystal structure, ground state and ionization energy, lattice constant, bulk modulus, crystal anharmonicity,[5] magnetic moments, and some photoemission spectra. However, there are also important limitations. For example, LDA predicts a band gap for semiconductors that is almost a factor of two too small, while the HFA overestimates the band gap for semiconductors.[6] In addition, for many strongly correlated (narrow energy band) systems such as high-temperature superconductors, heavy fermion materials, transition-metal oxides, and 3*d* itinerant magnets, the LDA is usually not sufficient for an accurate description (predicting metallic rather than semiconducting behavior, failing to predict quasiatomiclike satellites, etc).

Therefore, it is important to look for *ab initio* methods and improvements that go beyond LSDA. Recently there have been several attempts to combine *ab initio* LDA calculations with many-body approximations.[7–16] All of these recent developments add local, screened Coulomb (Hubbard) energies *U* between localized orbitals to the one-particle part of the Hamiltonian obtained from an *ab initio* LDA band-structure calculation, but differ in how they handle the correlation part. What these approaches have in common is that they have to introduce a Hubbard *U* as an additional param-

eter and hence are not really first-principles treatments. Although they use a LDA *ab initio* method to obtain a realistic band structure, i.e., single-particle properties, Coulomb matrix elements for any particular material are not known, and the Hubbard U remains an adjustable parameter. In addition, since some correlations are included in LDA as well as by the Hubbard U, it is unclear how to separate the two effects and double counting of correlation may be included in these approximations.

Other attempts to improve LDA include gradient corrections, nonlocal density schemes, self-interaction corrections, and the GW approximation (GWA), as defined below. Gradient corrections[17] approximately account for the fact that the electron density is not constant but $\mathbf{r}$ dependent in an inhomogeneous electron gas and use an exchange-correlation potential containing $\nabla n(\mathbf{r})$ terms. So-called generalized gradient approximation (GGA) functionals (e.g., Ref. 18) are now routinely used. The nonlocal density schemes go beyond LDA by considering that the exact exchange-correlation potential $V_{\mathrm{xc}}(\mathbf{r})$ cannot depend only on the density $n(\mathbf{r})$ at the same position $\mathbf{r}$ but should depend also on the electron density at all other positions $n(\mathbf{r}')$. Usually the new ansatz for the functional of the exchange-correlation energy contains the pair correlation function or the interaction of the electrons with the exchange-correlation hole.[17,19] The exact exchange (EXX) formalism[20–23] cancels the spurious (unphysical) electronic self-interaction present in LDA and gradient corrected exchange functionals. A standard method for *ab initio* calculations of excited states is the GWA.[24,25] Denoting the one-particle Green function by G and the screened interaction by W, the GWA is an approximation for the electronic self-energy $\Sigma \approx GW$, which is correct in linear order in W and can diagrammatically be represented by the lowest-order exchange (Fock) diagram. The one-particle Green function G is usually obtained for the effective one-particle LDA Hamiltonian.

The HFA has long been a standard electronic-structure method. Despite its many manifest defects, it is still important to know what such a calculation would predict before turning to more sophisticated approaches for correlation effects. In this paper we provide HFA calculations for Fe, Co, Ni, and Cu using an approach that we hope will be easily generalizable to more sophisticated treatments of correlation.

This is done by using the following steps:

(1) Perform a conventional, self-consistent, band-structure calculation for an effective one-particle Hamiltonian, namely, the Hartree Hamiltonian, to obtain a suitable basis set of Bloch functions.

(2) By taking into account only a finite number J of bands one chooses a truncated one-particle Hilbert space. The Marzari-Vanderbilt[26] algorithm is then used to construct a maximally localized set of Wannier functions, which span the same truncated one-particle Hilbert space.

(3) All one-particle (tight-binding) and two-particle (Coulomb) matrix elements of the Hamiltonian within this Wannier function basis are calculated.

(4) The resulting electronic many-body Hamiltonian in second quantization with parameters determined from first principles is studied within the HFA.

We use the ''linear muffin-tin orbital'' (LMTO) method[27] within the ''atomic-sphere approximation'' (ASA)[28] to perform the band-structure calculation for the Hartree Hamiltonian in first quantization. The second step of constructing localized Wannier functions is important, since then both the tight-binding and Coulomb matrix elements should be important only on-site and for a few neighbor shells (the most natural mapping to standard Hubbard-like models). The direct Coulomb matrix elements of the maximally localized Wannier basis are rather large, about 20 eV in magnitude. Our results are compared with those obtained from a standard LSDA calculation.[2,3,29,30] Although the $3d$ bands and the $4s$ band overlap in the LSDA approximation, our unscreened HFA calculations give $3d$ bands that lie considerably lower (between 10 and 20 eV) than the $4s$ band. The HFA correctly predicts ferromagnetism for the ferromagnetic metals Fe, Co, and Ni and no magnetism for Cu, but with a much larger exchange splitting between majority and minority $3d$ bands than obtained within LSDA and with a slightly larger magnetic moment per site than obtained experimentally or within LSDA. The total energy is lower in HFA than in LSDA. The LSDA results for metals are probably more reliable than our HFA results, which lack important screening and correlation effects. In order for our method to go beyond LSDA we would need to use better many-body methods than the (unscreened) HFA, which should be possible within our scheme.

To the best of our knowledge we do not know of any other published HFA results (band structure, density of states, magnetism, magnetic moment, total energy, etc.) for the $3d$ ferromagnets Fe, Co, and Ni, unless it was implicitly applied to these materials for schemes like the local ansatz,[31] where HFA results serve as an input to higher-order calculations. This is not surprising since the HFA has, from very early on, been viewed as a poor approximation for metals. For example, when applied to the homogeneous electron gas (as the simplest model of an infinite metallic system), the HFA has well-known Fermi edge singularities.[32,33] These lead, in particular, to a vanishing density of states (DOS) at the Fermi energy, which is, of course, unphysical. This unphysical feature, which is an effect of the long-range nature of the (unscreened) Coulomb term in the nonlocal exchange potential, usually prevails in actual HFA calculations for real metals,[34] though sometimes this singularity is hard to see in actual HFA results.[35] In our calculations the nonlocality is handled through the calculation of expectation values (matrix elements of the density matrix), which makes Hartree-Fock (HF) calculations as easy as Hartree calculations. Furthermore, because of our localized Wannier basis, we only keep on-site and next neighbor Coulomb and exchange matrix elements. Hence our calculations have an effective short-ranged Coulomb interaction. Although longer-range Coulomb matrix elements are small in our calculations, which is why we truncate them, it is possible that if all of them were kept to infinite distances that they could add up to give Fermi edge singularities (which are due to the long-ranged nature of the bare Coulomb interaction) and other standard anomalies. Correlation or screening would quickly kill these effects.

The approximation closest to HF is the EXX formalism[20–23] mentioned earlier. The method was first applied to atoms by Talman and Shadwick.[21] Later, the method was recognized as a DF method with EXX energy,[36] and applied to Si and Ge by Bylander and Kleinman in framework of the pseudopotential method.[37] The EXX method is different from the LDA only in that the EXX energy,[23] rather than the LDA exchange energy, is used; thus, LDA correlations are still present. The EXX energy, which corresponds to the Fock term in the HFA, is treated as a functional of electron density and the method is also (like HF) self-interaction-free. Although the EXX would appear to be very similar to HF, the EXX-only method,[38,39] which does not include any correlation, gives the dispersion of noninteracting electrons instead of the HF dispersion when applied to the homogeneous electron gas, while their total energies are exactly the same. For atoms the EXX-only method gives total energies that agree well with HF. Due to these similarities, we will compare our results with EXX where possible. One should note, however, that most EXX calculations include a local correlation potential.

The paper is organized as follows. In Sec. II, we briefly summarize some basic notation, give the Hamiltonian in first and second quantization, and describe our LMTO-Hartree calculations and our Wannier basis functions. Results for the matrix elements, in particular, the direct Coulomb and exchange matrix elements are given in Sec. III; we also compare these results with calculations of the Slater integrals. The application of the (unscreened) HFA to the multiband Hamiltonian in second quantization is the subject of Sec. IV. For an interpretation of the results we compare the numerical HFA results obtained for the crystal with previous atomic HFA results and with numerical and analytical results for a simplified local atomic model in Sec. V. A comparison with the more standard LSDA as well as EXX results follows in Sec. VI, before the paper closes with a short discussion.

II. HAMILTONIAN AND BASIS FUNCTIONS

A system of N_e interacting (nonrelativistic) electrons can be described by the Hamiltonian

$$H=T+V+W=\sum_{i=1}^{N_e}\frac{\mathbf{p}_i^2}{2m}+\sum_{i=1}^{N_e}V(\mathbf{r}_i)+\sum_{i>j}\frac{e^2}{|\mathbf{r}_i-\mathbf{r}_j|}. \quad (1)$$

The first part T is the kinetic energy of the electrons. The $V(\mathbf{r})$ describes the external one-particle potential. The formalism of ''second quantization,'' automatically accounts for the antisymmetry through the fermion anticommutation relations. In second quantization the full many-body Hamiltonian can be written as:

$$H=\sum_{i,j,\sigma}t_{ij}c_{i\sigma}^{\dagger}c_{j\sigma}+\frac{1}{2}\sum_{i,j,k,l,\sigma,\sigma'}W_{ij,kl}c_{i\sigma}^{\dagger}c_{j\sigma'}^{\dagger}c_{k\sigma'}c_{l\sigma}. \quad (2)$$

Here i,j,k,l denote a complete set of one-particle orbital quantum numbers and σ,σ' are the spin quantum numbers. The states $|i\rangle$ and the corresponding wave functions $\varphi_i(\mathbf{r})=\langle\mathbf{r}|i\rangle$ form a basis of the one-particle Hilbert space. The matrix elements in Eq. 2 of course depend on the one-particle basis $\{|i\rangle\}$ that is chosen. But because of the completeness relation the physical results should not depend on the choice of the one-particle basis. Because of the lattice periodicity an obvious choice for a one-particle basis is a Bloch basis $\{|n\mathbf{k}\rangle\}$; then the orbital one-particle quantum numbers $n,\mathbf{k}$ are the band index n and the wave number $\mathbf{k}$ (within the first Brillouin zone). In practice, one can work only on a truncated, finite-dimensional one-particle Hilbert space. Here the truncation consists of including only a finite number of bands and a set of $\mathbf{k}$ values from a discrete mesh in $\mathbf{k}$ space. But, because the Bloch states are delocalized, a very large number of Coulomb matrix elements (depending on four quantum numbers) between all possible $\mathbf{k}$ states would have to be calculated. Therefore, it seems that a more appropriate basis would be to use well localized wave functions, where it is expected that a short-range tight-binding assumption will hold, i.e., the on-site and the intersite matrix elements for only a few neighbor shells are sufficient. Wannier states (when maximally localized) are such wave functions. The Wannier states are related to the Bloch states by the unitary transformations:

$$w_{\mathbf{R}n}(\mathbf{r})=\langle\mathbf{r}|\mathbf{R}n\rangle=\frac{1}{N}\sum_{\mathbf{k}}e^{-i\mathbf{k}\mathbf{R}}\psi_{n\mathbf{k}}(\mathbf{r}),$$

$$|\psi_{n\mathbf{k}}\rangle=\sum_{\mathbf{R}}e^{i\mathbf{k}\mathbf{R}}|\mathbf{R}n\rangle. \quad (3)$$

Now our strategy is the following:

(i) Perform a traditional band-structure calculation for an effective one-particle Hamiltonian H_{eff} with lattice periodicity to obtain a Bloch basis of the Hilbert space. Only a finite number of band indices will be considered and the calculations will be done for a discretized, finite mesh in $\mathbf{k}$ space, i.e., we will work only on a reduced, truncated Hilbert space.

(ii) Determine well-localized Wannier functions spanning the same (truncated) Hilbert space as the Bloch basis from the canonical transformation (3) described above.

Of course, the important energy bands (and corresponding band indices) are those that determine the electronic properties of the system, i.e., the bands near to the Fermi level. Because the Hilbert space is truncated, we no longer work with a complete basis set. Hence, it is important to start from Bloch functions obtained from a band-structure calculation for a well-chosen effective one-particle Hamiltonian. The simplest choice would be the bare one-particle potential $V(\mathbf{r})$. However, without any Coulomb repulsion the $3d$ states become very strongly bound atomiclike (core) states, which would be pushed well below the Fermi energy, and therefore the corresponding Bloch eigenfunctions are not a good starting point to describe the electronic bands close to the Fermi level. Because the Hilbert space is truncated, it is extremely important to start from a band Hamiltonian $T+V_{\text{eff}}$ that gives eigenfunctions as close as possible to those which are expected to form the relevant many-body states of the interacting system. The bare one-particle potential is consequently a bad choice. Therefore, we choose the Hartree Hamiltonian, which already accounts for effects of the Cou-

TABLE I. Some properties of the lowest eight maximally localized Wannier functions of Fe.

n	0	1	2	3	4	5	6	7
$\Sigma_l C_l^{\mathbf{0}n}$	0.9761	0.9765	0.9596	0.9800	0.9773	0.8754	0.8731	0.8763
$\Sigma_{\mathbf{R}} C_{l=0}^{\mathbf{R}n}$	0.0019	0.0018	0.0081	0.0019	0.0017	.2224	0.2381	0.2265
$\Sigma_{\mathbf{R}} C_{l=1}^{\mathbf{R}n}$	0.0955	0.0726	0.1797	0.0611	0.0728	.5480	0.5509	0.5347
$\Sigma_{\mathbf{R}} C_{l=2}^{\mathbf{R}n}$	0.9026	0.9256	0.8121	0.9370	0.9255	.2295	0.2110	0.2388

lomb interaction in the mean-field approximation. Therefore, the eigenenergies (energy bands) will be about the right magnitude and the resulting basis functions can be expected to be more suitable in the energy regime around the Fermi level. Then the Bloch basis is obtained by solving the one-particle Schrödinger equation

$$\left[\frac{\mathbf{p}^2}{2m}+V(\mathbf{r})+V_{\mathrm{H}}(\mathbf{r})\right]\psi_{n\mathbf{k}}(\mathbf{r})=\varepsilon_n(\mathbf{k})\psi_{n\mathbf{k}}(\mathbf{r}), \tag{4}$$

where the Hartree potential is given by

$$V_{\mathrm{H}}(\mathbf{r})=\int d^3r'\frac{e^2n(\mathbf{r}')}{|\mathbf{r}-\mathbf{r}'|}. \tag{5}$$

Since the only purpose in solving the effective one-particle Schrödinger Eq. (4) is the construction of a suitable basis set of Bloch functions, we will not make use of the eigenenergies $\varepsilon_n(\mathbf{k})$ obtained in Eq. (4). Note that the Hartree potential, and hence our basis, is independent of spin. Nevertheless we can (in the following) expand the spin dependent HF Hamiltonian in this basis.

For the materials of interest we performed a self-consistent Hartree band-structure calculation. Besides the nuclear charge we used the (experimentally) known results for the lattice structure (bcc for Fe, fcc otherwise; Co should actually be hexagonal) and for the lattice constant as input. For the band-structure calculation we used the LMTO-ASA method of Refs. 27 and 28. We have used the frozen core approximation,[28] i.e., only treated the valence electrons as actual bands, while leaving the core electrons ''frozen.'' For the radius of the overlapping muffin-tin spheres, the Wigner-Seitz radius S, we used: $S=2.662a_0$ for Fe, $S=2.621a_0$ for Co, $S=2.602a_0$ for Ni and $S=2.669a_0$ for Cu (Ref. 28). Within the muffin-tin spheres the potential and wave functions are expanded in spherical harmonics with a cutoff $l_{\max}=2$, i.e., s, p, and d orbitals are included, which limits the calculation to nine bands for one atom per unit cell.

In Ref. 40, we describe how maximally localized Wannier functions can be calculated from LMTO Bloch wave functions using a method proposed by Marzari and Vanderbilt, which is described in detail in Ref. 26. The Wannier functions are admixtures having different angular contributions ($3d$, $4s$, $4p$). Since the original Bloch functions from which the Wannier functions are constructed were given in terms of a spherical harmonics expansion, the new Wannier functions (and their contribution in each individual muffin-tin sphere) can also be decomposed into these spherical harmonics contributions

$$w_n(\mathbf{R};\mathbf{r})=\sum_L\{\phi_{\nu l}(r)A_L^{\mathbf{R}n}+\dot{\phi}_{\nu l}(r)B_L^{\mathbf{R}n}\}Y_L(\hat{\mathbf{r}}). \tag{6}$$

Here, the $\phi_{\nu l}(r)$'s are normalized radial basis functions and $\dot{\phi}_{\nu l}(r)$ are their energy derivatives for an energy $E_{\nu l}$; this is a standard notation in the LMTO method (see Ref. 28). One can then calculate the weight of the contributions to the Wannier function (centered at $\mathbf{0}$) within the different muffin-tin spheres

$$\langle w_n|w_n\rangle_{\mathbf{R}}\equiv\int_{\mathbf{R}}d^3\mathbf{r}|w_n(\mathbf{r})|^2=\int_{\mathbf{0}}d^3\mathbf{r}|w_n(\mathbf{R};\mathbf{r})|^2, \tag{7}$$

and one can also decompose this into the different l contributions according to

$$\langle w_n|w_n\rangle_{\mathbf{R}}=\sum_l\underbrace{\sum_{m=-l}^{l}\{|A_{lm}^{\mathbf{R}n}|^2+\langle\dot{\phi}_{\nu l}^2\rangle|B_{lm}^{\mathbf{R}n}|^2\}}_{\equiv C_l^{\mathbf{R}n}}. \tag{8}$$

For the $3d$ system iron these quantities are tabulated in Table I. The first line is the weight $\langle w_n|w_n\rangle_{\mathbf{0}}$ in the center muffin tin. Between 88 and 98 % of the total weight of the Wannier functions is to be found already within the center muffin tin; this shows how well localized our Wannier functions are with the lowest five functions having values of more than 95%. Rows 2–4 in this table indicate the different l contribution or l character of the Wannier functions. One sees that the optimally localized Wannier functions are not pure within their l character, but the lowest five Wannier functions (0–4) still have mainly $l=2$ ($3d$) character. Higher band-index states (which are slightly less well localized according to row 1) are admixtures that have mainly $l=1$ ($4p$) character (about 50%), but also a considerable amount of $l=0$ ($4s$) and $l=2$ ($3d$) character. Corresponding results for the other $3d$ systems Co, Ni, and Cu are similar and, therefore, not repeated here. Our detailed results are given in Ref. 30.

III. ONE PARTICLE AND COULOMB MATRIX ELEMENTS

From the optimally localized Wannier functions we calculate the one-particle matrix elements

$$t_{12}=\int d^3\mathbf{r}\;\; w_1^*(\mathbf{r})\left[-\frac{\hbar^2}{2m}\boldsymbol{\nabla}^2+V(\mathbf{r})\right]w_2(\mathbf{r}), \tag{9}$$

and the Coulomb matrix elements of the Hamiltonian

TABLE II. On-site direct and exchange Coulomb matrix elements between Wannier functions for Fe. All energies are in eV's.

U_{nm}	0	1	2	3	4	5	6	7	8
0	22.42	20.90	20.10	20.96	20.86	14.16	13.32	13.96	13.50
1	20.90	23.04	19.95	21.55	21.53	14.07	13.54	13.58	14.15
2	20.10	19.95	20.77	20.05	19.83	12.95	13.46	13.37	13.22
3	20.96	21.55	20.05	23.27	21.67	13.46	14.05	13.98	13.98
4	20.86	21.53	19.83	21.67	22.99	13.71	13.28	14.25	14.12
5	14.16	14.07	12.95	13.46	13.71	13.67	9.45	9.58	9.64
6	13.32	13.54	13.46	14.05	13.28	9.45	13.52	9.27	9.50
7	13.96	13.58	13.37	13.98	14.25	9.58	9.27	13.75	9.65
8	13.50	14.15	13.22	13.98	14.12	9.64	9.50	9.65	13.81
J_{nm}	0	1	2	3	4	5	6	7	8
0	22.42	0.84	0.61	0.75	0.99	0.86	0.73	0.81	0.42
1	0.84	23.04	0.77	0.88	0.84	0.70	0.51	0.48	0.86
2	0.61	0.77	20.77	0.88	0.70	0.96	0.93	0.92	0.60
3	0.75	0.88	0.88	23.27	0.82	0.33	0.78	0.64	0.69
4	0.99	0.84	0.70	0.82	22.99	0.52	0.46	0.75	0.83
5	0.86	0.70	0.96	0.33	0.52	13.67	0.58	0.56	0.57
6	0.73	0.51	0.93	0.78	0.46	0.58	13.52	0.45	0.56
7	0.81	0.48	0.92	0.64	0.75	0.56	0.45	13.75	0.55
8	0.42	0.86	0.60	0.69	0.83	0.57	0.56	0.55	13.81

$$W_{12,34}=\int d^3\mathbf{r}\ d^3\mathbf{r}'\ \ w_1^*(\mathbf{r})\ \ w_2^*(\mathbf{r}')\times\frac{e^2}{|\mathbf{r}-\mathbf{r}'|}\ \ w_3(\mathbf{r}')\ \ w_4(\mathbf{r}). \tag{10}$$

Here we use the abbreviated notation 1 to mean $\mathbf{R}_1 n_1$ and 2 to mean for $\mathbf{R}_2 n_2$, etc. In Ref. 40, we have described how these matrix elements can be evaluated. Concerning the Coulomb matrix elements, we have used the two different numerical algorithms proposed in Ref. 40 for their evaluation, namely the FFT algorithm and a spherical expansion algorithm. The latter method makes use of the fact that (in each muffin-tin sphere) the Wannier functions are explicitly given as linear combinations of products of spherical harmonics and a radial wave function. The expansion

$$\frac{1}{|\mathbf{r}-\mathbf{r}'|}=\sum_{k=0}^{\infty}\frac{4\pi}{2k+1}\frac{r_<^k}{r_>^{k+1}}\sum_{m=-k}^{k}Y_K^*(\hat{\mathbf{r}}')\ Y_K(\hat{\mathbf{r}}) \tag{11}$$

($K=\{k,m\}$) makes it possible to express the on-site Coulomb integrals as one-dimensional integrals over products of the radial functions and Gaunt coefficients. The results obtained by this algorithm and by the independent FFT algorithm agree within errors of atmost 1%. Since our basis functions are well localized, we may truncate the tight-binding and Coulomb matrix elements. We only consider on-site and next neighbor matrix elements, by next neighbor Coulomb matrix elements, we mean matrix elements for which the four sites (appearing in the indices) are (pairwise) maximally a next neighbor distance apart.

Results for the on-site direct and exchange Coulomb matrix elements between the optimally localized Wannier functions are given in Table II for iron. The direct Coulomb integrals $U_{nm}=W_{nm,mn}$ between the Wannier states with the lowest five band indices ($n,m\in\{0,\ldots,4\}$), which according to Table I have mainly $3d$ character are rather large, up to 23 eV for Fe. Within the $3d$-like bands the interband direct Coulomb matrix elements are of the same magnitude as the intraband matrix elements. The matrix elements between $3d$ states and $4sp$ states are considerably smaller, of the magnitude of 13–14 eV. For electrons in $4sp$ states ($n,m\in\{5,\ldots,9\}$) the direct intraband Coulomb matrix elements are again of the order of 13–14 eV, but the interband matrix elements are slightly smaller, about 9 eV. The exchange matrix elements $J_{nm}=W_{nm,nm}$ are always much smaller, usually less than 1 eV (for $n\neq m$). The corresponding results for the other $3d$ systems investigated (Co, Ni, and Cu) are very similar.[30]

For the five states with predominant $3d$ character we have calculated the averages of the on-site direct and exchange Coulomb matrix elements

$$U\equiv\frac{1}{25}\sum_{mm'}W_{mm'm'm}, \tag{12}$$

$$J\equiv\frac{1}{20}\sum_{m\neq m'}W_{mm'mm'}, \tag{13}$$

as well as the averages of the absolute values of the nearest-neighbor (NN) and next-nearest-neighbor (NNN) hopping matrix elements

TABLE III. Averaged on-site Coulomb, exchange, nearest neighbor, and next-nearest-neighbor hopping matrix elements for the four $3d$ systems; energies are in eV.

	U	J	t_{NN}	t_{NNN}
Fe	21.1	0.81	0.59	0.24
Co	22.6	0.87	0.55	0.10
Ni	22.6	0.88	0.75	0.11
Cu	24.5	0.94	0.80	0.12

$$t_{NN(N)} \equiv \frac{1}{25} \sum_{n,m} |t_{\mathbf{R}nm}|. \tag{14}$$

The results obtained thereby for the four transition metals under consideration are shown in Table III. The U values vary between 21 eV for Fe and 25 eV for Cu, the J values are smaller than 1 eV and the hopping matrix elements are of the magnitude 0.5–0.7 eV for NN and 0.1–0.2 eV for NNN, and further on decrease with increasing distance.

We have also evaluated the Slater integrals:[41]

$$F^k \equiv e^2 \int dr\ r^2 \int dr'\ r'^2\ |R_{l=2}(r)|^2\ \frac{r_<^k}{r_>^{k+1}}\ |R_{l=2}(r')|^2, \tag{15}$$

where $R_{l=2}(r)$ is a radial (atomic) d-wave function (obtained by solving the Schrödinger equation for a radial symmetric potential, for instance). Note that only the three integrals F^0, F^2, and F^4 are required to determine all the Coulomb d-matrix elements. Using the radial d-wave function obtained from the Hartree calculation we obtain the following values for the Slater integrals of the four $3d$ systems: $F^0 = 21.62$ eV for Fe, 23.18 eV for Co, 24.69 eV for Ni, and 26.27 eV for Cu. This means that the Slater integrals F^0 are rather good estimates of our (averaged) Coulomb matrix elements. These values are also in agreement with older results obtained in calculations for $3d$ atoms.[42] In Table IV we show our F^k values for the four $3d$ crystals and compare them with corresponding atomic calculations from Ref. 42. Obviously, there is fairly good agreement between these atomic calculations and our results.

TABLE IV. Slater integrals F^k (in eV) for the $3d$ systems Fe, Co, Ni, Cu as obtained by our calculations and within an earlier atomic calculation.[42]

	F^0	F^2	F^4
Fe (crystal)	21.62	9.61	5.91
Fe (atom [42])	23.76	10.96	6.81
Co (crystal)	23.18	10.31	6.34
Co (atom [42])	25.15	11.58	7.20
Ni (crystal)	24.69	11.00	6.77
Ni (atom [42])	26.53	12.20	7.58
Cu (crystal)	26.27	11.72	7.23
Cu (atom [42])	27.90	12.82	7.96

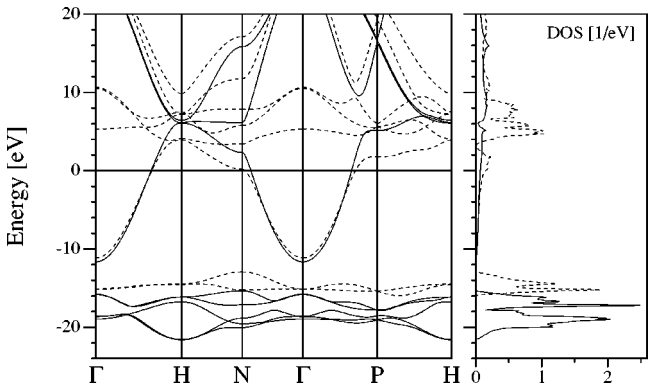

FIG. 1. Hartree-Fock band structure and density of states (per spin) of Fe; the full line shows the majority (spin up), the dashed line shows the minority spin component.

IV. UNSCREENED HARTREE-FOCK APPROXIMATION

After we have determined the matrix elements within our restricted basis set of nine maximally localized Wannier functions (per site and spin), we have a Hamiltonian in second quantization of the form

$$H = \sum_{12\sigma} t_{12} c_{1\sigma}^\dagger c_{2\sigma} + \frac{1}{2} \sum_{1234\sigma\sigma'} W_{12,34} c_{1\sigma}^\dagger c_{2\sigma'}^\dagger c_{3\sigma'} c_{4\sigma} \tag{16}$$

for which all the matrix elements are known from first principles. The simplest approximation one can now apply is the HFA, which replaces the many-body Hamiltonian by the effective one-particle Hamiltonian

$$H_{\mathrm{HF}} = \sum_{12\sigma} (t_{12} + \Sigma_{12,\sigma}^{\mathrm{HF}}) c_{1\sigma}^\dagger c_{2\sigma}, \tag{17}$$

with

$$\Sigma_{12,\sigma}^{\mathrm{HF}} = \Sigma_{12}^{\mathrm{Hart}} + \Sigma_{12,\sigma}^{\mathrm{Fock}} = \sum_{34\sigma'} [W_{13,42} - \delta_{\sigma\sigma'} W_{31,42}] \langle c_{3\sigma'}^\dagger c_{4\sigma'} \rangle. \tag{18}$$

Here the expectation values $\langle c_{1\sigma}^\dagger c_{2\sigma} \rangle$ have to be determined self-consistently for the HF Hamiltonian (17). Note that the

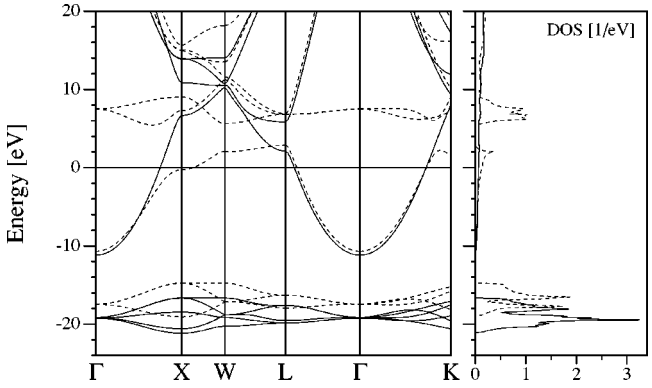

FIG. 2. Hartree-Fock band structure and density of states (per spin) of Co; the full line shows the majority (spin up), the dashed line shows the minority spin component.

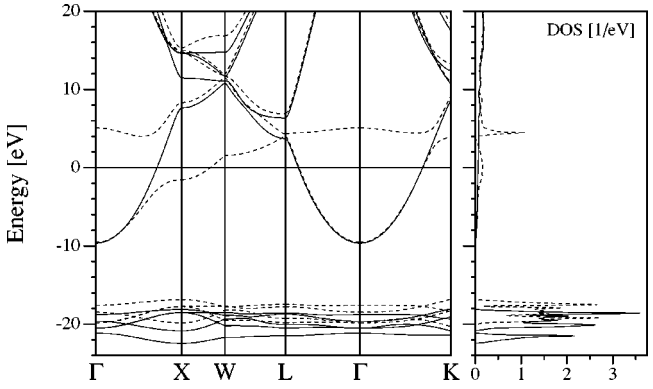

FIG. 3. Hartree-Fock band structure and density of states (per spin) of Ni; the full line shows the majority (spin up), the dashed line shows the minority spin component.

Fock (exchange) term is spin σ dependent and may, therefore, give rise to magnetic solutions.

The Hartree-Fock results for the four materials of interest are shown in Figs. 1–4. We show the effective HF band structure and its density of states (DOS). In our HF calculations there are no singularities (or a vanishing DOS) at the Fermi level since we start from a localized description and consider the Coulomb matrix elements only up to next neighbors. Therefore, we implicitly truncate the Coulomb interaction in real space and in practice work with an effective short-ranged interaction. Within HFA the main part of the $3d$ bands lies between 18 and 22 eV below the Fermi level and is separated from the $4sp$ bands. We find magnetism in HFA for Fe, Co, and Ni in agreement with experiment. The five majority spin d bands are about 20 eV below the Fermi energy and are completely filled. But the partially filled minority d bands have two (for Fe), three (for Co), and four (for Ni) filled bands between -18 and -15 eV, and the rest are around and above the Fermi level. The resulting magnetic moments are shown in Table V. For copper no magnetism and exchange splitting of the $3d$ bands is obtained, but the (spin degenerate) $3d$ bands are at about 22 eV below the Fermi level and separated from the $4sp$ bands. If we compare these results with the results of the simple Hartree approximation, which are qualitatively similar to LDA results (as shown, e.g., in Ref. 29, or in our detailed results[30]), we see that the exchange term has two effects: It produces an exchange splitting and the possibility of magnetic solutions, and it draws the $3d$ bands energetically down by an amount of about 20 eV. Compared with experiment the HFA overestimates magnetism and leads to overly large values for the magnetic moment, see Table V. This is consistent with Heisenberg or Ising model studies where the mean-field approximation HFA also has the tendency to overestimate magnetism and magnetic solutions. However, the reason why the $3d$ bands lie so far below the Fermi level and the $4sp$ band in HFA has nothing to do with the existence and overestimation of magnetism. This can be seen already from the nonmagnetic system Cu for which the (fully occupied) $3d$ bands also lie at about 22 eV below the Fermi level (see Fig. 4). To demonstrate this also for a system with a partially filled $3d$ band we have done a nonmagnetic Hartree-Fock calculation for Co (by forcing equal occupation for both spin directions). The results for the band structure and the DOS are shown in Fig. 5. We observe again that the main part of the $3d$ bands are well below the $4s$ bands and Fermi level; note the hybridization gap caused by the unoccupied $3d$ bands above the Fermi level.

TABLE V. Spin magnetic moments (μ_B/atom) from different methods. The EXX results are from Ref. 45.

	HF	EXX	LSDA	Experiment
Fe	2.90	3.27	2.18	2.22
Co	1.90	2.29	1.58	1.72
Ni	0.76	0.68	0.58	0.62

V. COMPARISON WITH ATOMIC HARTREE-FOCK RESULTS

We have seen in the preceding section that one effect of the HFA calculation, when compared with the Hartree calculation, is the shift of the $3d$ bands down (about 20 eV below the Fermi level and about 8–10 eV below the bottom of the $4sp$ band). This shift of the d bands is about the same energy as the Coulomb matrix elements U, and roughly agrees with earlier atomic Hartree-Fock calculations,[42,43] where the $3d$ states are also about 10 eV below the $4s$ states.

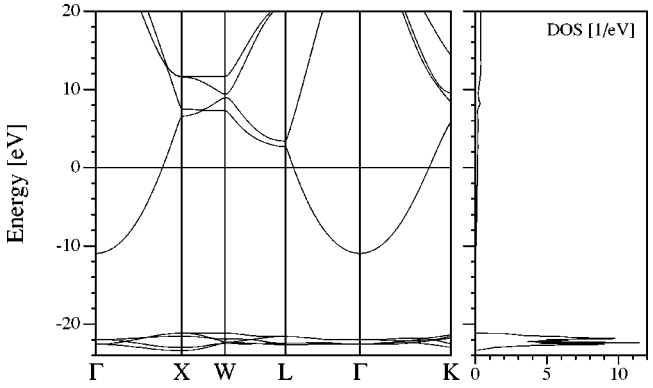

FIG. 4. Hartree-Fock band structure and density of states (for both degenerate spin directions) of Cu.

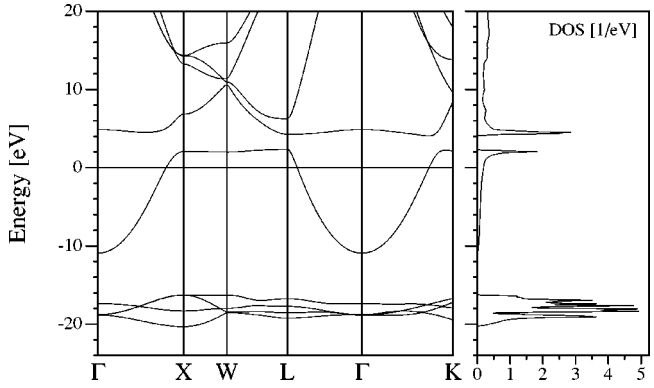

FIG. 5. Nonmagnetic Hartree-Fock band structure and density of states (for both degenerate spin directions) of Co.

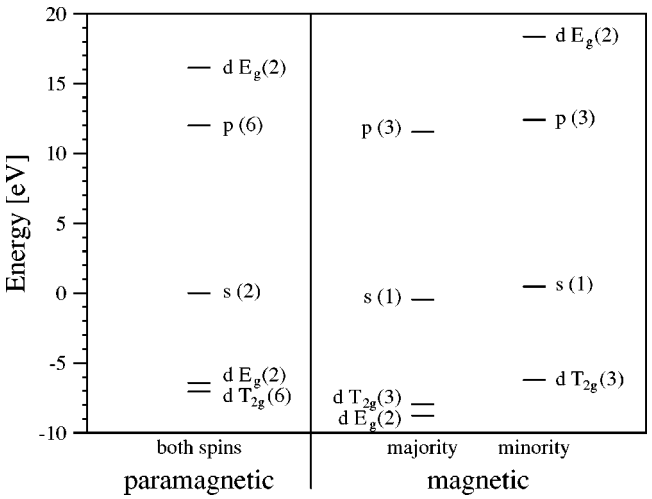

FIG. 6. Energy eigenvalues from quasiatomic HFA calculation. The numbers in brackets indicate the degeneracy.

Because the intersite hopping matrix elements in Table III are much smaller than the U values one may consider an expansion in t/U, with the zeroth-order approximation to completely neglect hopping. Doing this, we have performed a quasi-atomic HFA calculation for Co, by including only the on-site one-particle and two-particle (Coulomb) matrix elements. The results are summarized in Fig. 6; the degeneracy of the different levels is also indicated. In the paramagnetic case, we find that the $3d$ bands are below the $4s$ bands (at the Fermi level) by about 6 to 7 eV, which is in rough agreement with the earlier atomic HFA results.[42,43] The splitting between the occupied and unoccupied $3d$ states is about 23 eV, which is the on-site U for Co. Magnetic HFA solutions are also found in the atomic limit for Co, as shown in the right panel of Fig. 6. The majority-spin $3d$ states (T_{2g} and E_g) are now completely filled and energetically lie lower than the corresponding nonmagnetic HFA states. But only the (threefold degenerate) T_{2g} states of the minority-spin electrons are filled whereas the E_g states of the minority electrons are empty (and now even 26 eV above the occupied d states). The additional energetical shifts between the occupied $3d$ states in the paramagnetic and ferromagnetic atomic HFA solution are due to the exchange matrix elements J.

This behavior can qualitatively be understood within the framework of the following simple, analytically solvable model. Similar to the numerical HFA results presented and discussed above, we neglect all intersite one-particle (hopping) and interaction matrix elements. Furthermore, we assume that we have diagonalized the one-particle Hamiltonian taking into account only the atomic $3d$ levels and assuming that the on-site one-particle diagonal matrix elements ε, the Coulomb matrix elements U, and the exchange matrix elements J are equal, i.e., the $3d$ levels are degenerate in the atomic limit with no crystal-field effects. Then the atomic part of the many-body Hamiltonian can be written as

$$H=\sum_{i\sigma}\ \varepsilon\ \ c_{i\sigma}^{\dagger}c_{i\sigma}+\frac{U}{2}\sum_{(i\sigma)\neq(j\sigma')}c_{i\sigma}^{\dagger}c_{i\sigma}c_{j\sigma'}^{\dagger}c_{j\sigma'}+\frac{J}{2}\sum_{i\neq j,\sigma\sigma'}c_{i\sigma}^{\dagger}c_{j\sigma'}^{\dagger}c_{i\sigma'}c_{j\sigma}, \tag{19}$$

where $i,j\in\{0,\ldots,4\}$ denote the five (degenerate) $3d$ states.

Assuming that no symmetry breaking occurs and that off-diagonal expectation values $\langle c_{j\sigma'}^{\dagger}c_{i\sigma}\rangle$ for $(i\sigma)\neq(j\sigma')$ vanish, the standard HFA decoupling leads to the following effective one-particle Hamiltonian

$$H=\sum_{i\sigma}\ \varepsilon_{i\sigma}^{\mathrm{HFA}}c_{i\sigma}^{\dagger}c_{i\sigma}, \tag{20}$$

where

$$\varepsilon_{i\sigma}^{\mathrm{HFA}}=\varepsilon+U\left[\sum_{j\sigma'}\ \langle c_{j\sigma'}^{\dagger}c_{j\sigma'}\rangle-\langle c_{i\sigma}^{\dagger}c_{i\sigma}\rangle\right]-J\sum_{j\neq i}\ \langle c_{j\sigma}^{\dagger}c_{j\sigma}\rangle. \tag{21}$$

Obviously, in this atomic HFA treatment starting from localized orbitals the self-interaction is exactly canceled. In the simple Hartree approximation (HA) the exchange decouplings are neglected, which means that all the decoupling terms with the negative sign would not occur. Therefore, the corresponding Hartree one-particle energies are given by

$$\varepsilon_{i\sigma}^{\mathrm{HA}}=\varepsilon+U\sum_{j\sigma'}\ \langle c_{j\sigma'}^{\dagger}c_{j\sigma'}\rangle. \tag{22}$$

Comparing this result with the Hartree-Fock one-particle energies, we find that the HF occupied levels are shifted downwards by an amount of

$$U\langle c_{i\sigma}^{\dagger}c_{i\sigma}\rangle+J\sum_{j\neq i}\ \langle c_{j\sigma}^{\dagger}c_{j\sigma}\rangle \tag{23}$$

relative to the Hartree levels. Momentarily setting $J=0$, we see that for N occupied levels the Hartree approximation gives the one-particle energies

$$\varepsilon_{i\sigma}^{\mathrm{HA}}=\varepsilon+NU, \tag{24}$$

whereas the HFA yields

$$\varepsilon_{i\sigma}^{\mathrm{HFA}}=\varepsilon+(N-1)U. \tag{25}$$

The occupied Hartree-Fock one-particle energies are lower than the corresponding Hartree one-particle energies by U, which is a consequence of the artificial and unphysical self-interaction still present in the Hartree approximation that is exactly canceled in Hartree-Fock. This also explains why the Hartree-Fock bands are shifted downwards from the Hartree bands by an energy of the amount U. One also sees from this simple atomic-limit Hartree-Fock model that the energy difference between the highest occupied and the lowest unoccupied effective Hartree-Fock one-particle energies is again essentially U, which is once more in agreement with our numerical results for the crystal and for the atom (cf. Fig. 6). Note that we have ignored U_{sd} interactions, which cause an additional shift of d bands below the s bands by about an additional 10 eV in the full HFA calculations.

Taking into account the exchange interaction J again and denoting by N_{σ} the number of occupied states with spin σ (i.e., $N=N_{\uparrow}+N_{\downarrow}$) one obtains in HFA

$$\varepsilon_\sigma^{\mathrm{HFA}} = \varepsilon + (N-1)U - (N_\sigma - 1)J. \tag{26}$$

Then the total energy in HFA is given by

$$E_{\mathrm{tot}} = N\varepsilon + \frac{N(N-1)}{2}U - \sum_\sigma \frac{N_\sigma(N_\sigma-1)}{2}J. \tag{27}$$

For the total energy we have added the necessary correction term to the sum of the occupied energy levels (much like the double counting term that shows up in band-structure calculations). Now for partially filled $3d$ shells the occupation of the different spin directions may be different. Denoting $M = N_\uparrow - N_\downarrow$ we obtain for the total energy

$$E_{\mathrm{tot}} = N\varepsilon + \frac{N(N-1)}{2}U - \frac{N^2+M^2}{4}J + \frac{N}{2}J. \tag{28}$$

The magnetic ($M \neq 0$) total energy is lower than the nonmagnetic (consistent with Hund's rules).

Take once more Co with eight $3d$ electrons. The paramagnetic (nonmagnetic) state has the occupations $N_\downarrow = N_\uparrow = 4$ ($N=8$ and $M=0$). For this configuration (corresponding to the left panel in Fig. 6) one obtains

$$E_{\mathrm{tot}}^{(P)} = 8\varepsilon + 28U - 12J. \tag{29}$$

The Hund's rule magnetic solution has $3d$ states of one spin direction completely filled, i.e., $N_\uparrow = 5$ and $N_\downarrow = 3$ ($N=8$ and $M=2$). This gives

$$E_{\mathrm{tot}}^{(M)} = 8\varepsilon + 28U - 13J. \tag{30}$$

Therefore, the magnetic configuration (with a magnetic moment of 2 for the atom) is energetically more favorable by J. Note also the exchange splitting in the occupied energy eigenvalues

$$\varepsilon_\downarrow - \varepsilon_\uparrow = 2J \tag{31}$$

and that our model would predict the unoccupied minority spin E_{2g} state to be $U+J$ higher in energy than the corresponding occupied majority spin state.

The simple model in this section differs from the results shown in Fig. 6 in that we have replaced the full matrix of U and J by scalar values for d states only (ignoring s-d interactions, for example). However, it captures all of the important physics without attempting to be completely quantitative.

VI. COMPARISON WITH LSDA AND EXX RESULTS

For comparison with the HFA results described in Sec. IV we have also performed a standard LSDA band-structure calculation with the LMTO-ASA method. We used the von Barth–Hedin exchange-correlation potential.[44] Since these results are very similar to those of Ref. 29, we do not repeat them here. Again, our detailed results are given in Ref. 30. For the magnetic systems Fe, Co, and Ni we obtain an exchange splitting and the prediction of magnetic solutions with magnetic moments shown in Table V, which are in better agreement with experiment than the HFA results.

The energy spectra of the bands (DOS) are quite different from the HFA. For example, the $3d$ bands now fall into the same energy region as the $4sp$ bands, i.e., the LSDA results are not so different from the Hartree results. This means that the exchange-correlation energy leads only to a small shift of the $3d$ bands downwards by atmost a few electron volts and a smaller exchange splitting (also of the magnitude of 1 eV). On the other hand, in the LSDA calculations the self-interaction terms are not completely canceled, i.e., an (unrealistic) self-interaction is included, which may lead to $3d$ bands that lie energetically too high, as discussed for the atomic limit in the preceding section.

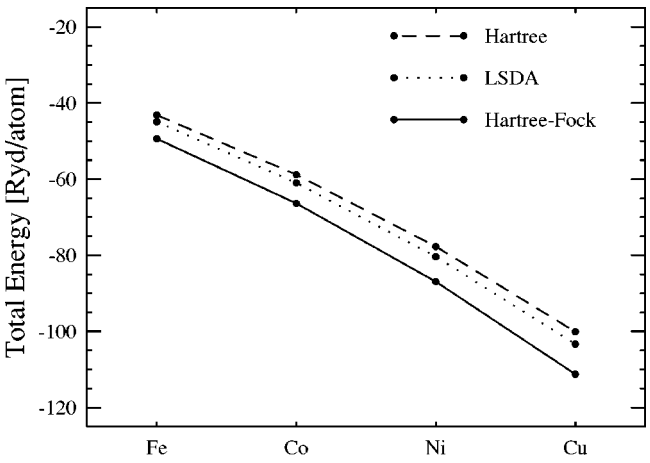

FIG. 7. Total ground-state energy (of the valence electrons) obtained in Hartree approximation, LSDA, and HFA for the $3d$ transition metals Fe through Cu.

To see the effect of correlations within LSDA, we have also performed an exchange-only calculation for Co, i.e., only the exchange part of the (local) exchange-correlation potential[44] was employed. The result is similar to the LSDA result, and the (majority) d bands lie only about 1 eV lower than within LSDA, i.e., very minimal when compared with the large drop in the full HFA. This exchange-only LSDA result also contains self-interactions, and their exact cancellation in the HFA is responsible for the large shift downwards of the d bands. Nevertheless, the LSDA result indicates that a possible effect of correlations is to shift the $3d$ bands up relative to exchange-only calculations, and hence one would expect a similar effect if correlations could be added to the full HFA calculations.

One can also calculate the total energy in the Hartree, HFA, and LSDA approximations. The results obtained for the four materials of interest are shown in Fig. 7. We see that the total energy is always significantly lower in HFA than in the Hartree approximation, which is expected because the HFA uses a better variational wave function. The HFA total energy is also lower than the LSDA, and the LSDA result is lower than the simple Hartree result. Because of the unknown approximations that go into constructing LSDA, it is hard to guess ahead of time that this would be the case. However, it is well known that the LSDA approximation produces a bad total exchange-correlation energy; the reason why such good agreement with experiment is found is that relative exchange-correlation energies are nonetheless reasonably accurately calculated.

We now turn to the comparison of our results with EXX calculations for $3d$ systems.[23,45] This method, which is self-interaction-free, uses the EXX energy[23] instead of a LDA exchange and then adds in a LDA correlation potential. Like the HFA the magnetic moments for Fe, Co, and Ni (see Table V) are overestimated by EXX.[45] Our HFA results for Fe show the majority $3d$ bands about 20 eV below the Fermi level (Fig. 1), whereas the EXX density of states (Fig. 2 in Ref. 23) show these bands only about 10 eV below the Fermi level. The differences are probably due to the (LDA) correlations shifting the $3d$ bands upwards. This upward shift also occurs with EXX+RPA (random-phase approximation) results in Ref. 45. Here the LDA correlations present in EXX are replaced by RPA correlations and the $3d$ bands are found in the region of the $4sp$ bands (similar to LDA). It is likely that the qualitative agreement between the HFA and EXX results for Fe is due to the correct cancellation of self-interactions.

VII. DISCUSSION AND CONCLUSION

We have presented the results of (unscreened) HFA calculations for the $3d$ transition metals Fe, Co, Ni, and Cu. We obtain magnetic solutions for Fe, Co, and Ni with (slightly) too large magnetic moments when compared to experimental or LSDA results. The occupied HFA $3d$ bands lie about 20 eV below the Fermi level (and the Hartree result), which is also the magnitude of the splitting between occupied and unoccupied $3d$ bands and of the magnitude of the on-site Coulomb matrix element (the ''Hubbard'' U). This downwards shift of the HFA $3d$ bands compared to the Hartree and LSDA $3d$ bands can be understood as due to the self-interaction correction of HFA.

One may argue that these results are not surprising and an artifact of using the unscreened HFA. Our *ab initio* calculation of the direct Coulomb matrix elements yields large values of the magnitude of 20 eV. HFA can be considered to be an approximation for the self-energy which is correct only in linear order in the Coulomb interaction. But for these large values of the U terms HFA is certainly not sufficient but one has to apply better many-body approximations. One should apply systematic extensions of HFA, which within the standard perturbational approach can be represented by (a resummation of an infinite series of) Feynman diagrams, or one can try to apply the recently so successful nonperturbational many-body schemes like ''dynamical mean-field theory'' (DMFT)[46] or variational (Gutzwiller) approaches.[47] The simplest standard diagram series are the bubble diagrams leading essentially to the ''random-phase approximation'' (RPA). This means just a renormalization of the interaction line, i.e., the pure ''naked'' Coulomb interaction has to be replaced by a ''dressed'' interaction. Or in other words, the exchange (Fock) contribution has not to be calculated with the bare Coulomb matrix elements but with screened Coulomb matrix elements. Probably the nonperturbational schemes like DMFT are also only applicable for screened Coulomb matrix elements.

We believe that the approach we have used for our HFA calculations can easily be generalized to provide an approach for combining *ab initio* and many-body methods for the calculation of the electronic properties of solids. The starting point is a traditional band-structure calculation for an effective (auxiliary) one-particle Hamiltonian, which can be the Hartree Hamiltonian. This yields, in particular, the eigenfunctions in the form of Bloch functions. Keeping only a finite number of J band indices restricts and truncates the Hilbert space for further calculations. We use the Marzari-Vanderbilt algorithm to construct maximally localized Wannier functions (within the truncated one-particle Hilbert space). All the one-particle (tight-binding) and two-particle (Coulomb) matrix elements between these Wannier functions can be calculated. The strong localization guarantees that only on-site matrix elements and near neighbor intersite matrix elements have to be calculated. We are left with a many-body Hamiltonian in second quantization but with parameters determined from first principles for any given material, which we have solved within the HFA but for which we should also be able to solve by using more sophisticated many-body techniques. Our HFA approach is free from the problems of double counting of correlation effects and self-interaction and considers exchange contributions exactly. It does not rely on assumptions based on the homogeneous electron gas or a dependence on the local electron density. An inhomogeneous (lattice) electron system is considered right from the beginning. Within the standard Feynman diagram approach the most straightforward next step beyond HFA would be a summation of bubble diagrams leading to a renormalized (screened) Coulomb interaction. This would require calculating the exchange contribution not with the bare but with a screened Coulomb interaction. To take into account the effects of screening would require a calculation of the charge susceptibility and the (static) dielectric constant, which could be done within a generalized Lindhard theory, for instance.

ACKNOWLEDGMENTS

This work has been supported by a grant from the Deutsche Forschungsgemeinschaft Grant No. Cz/31-12-1. It was also partially supported by the Department of Energy under Contract No. W-7405-ENG-36. This research used resources of the National Energy Research Scientific Computing Center, which is supported by the Office of Science of the U.S. Department of Energy under Contract No. DE-AC03-76SF00098.

[1] P. Hohenberg and W. Kohn, Phys. Rev. **136**, B864 (1964).
[2] R.M. Dreizler and E.K.U. Gross, *Density Functional Theory* (Springer, Berlin, 1990).
[3] H. Eschrig, *The Fundamentals of Density Functional Theory* (Teubner Stuttgart, Leipzig, 1996).
[4] W. Kohn and L.J. Sham, Phys. Rev. **140**, A1133 (1965).
[5] J.H. Rose, J.R. Smith, F. Guinea, and J. Ferrante, Phys. Rev. B **29**, 2963 (1984).
[6] A. Svane, Phys. Rev. B **35**, 5496 (1986).
[7] V.I. Anisimov, J. Zaanen, and O.K. Andersen, Phys. Rev. B **44**, 943 (1991).
[8] M.M. Steiner, R.C. Albers, D.J. Scalapino, and L.J. Sham, Phys. Rev. B **43**, 1637 (1991).
[9] M.M. Steiner, R.C. Albers, and L.J. Sham, Phys. Rev. B **45**, 13 272 (1992); Phys. Rev. Lett. **72**, 2923 (1994).
[10] V.I. Anisimov, A.I. Poteryaev, M.A. Korotin, A.O. Anokhin, and G. Kotliar, J. Phys.: Condens. Matter **9**, 7359 (1997).
[11] A.I. Lichtenstein and M.I. Katsnelson, Phys. Rev. B **57**, 6884 (1998).
[12] V. Drchal, V. Janis, and J. Kudrnovsky, Phys. Rev. B **60**, 15 664 (1999).
[13] M.I. Katsnelson and A.I. Lichtenstein, J. Phys.: Condens. Matter **11**, 1037 (1999).
[14] A. Liebsch and A. Lichtenstein, Phys. Rev. Lett. **84**, 1591 (2000).
[15] T. Wegner, M. Potthoff, and W. Nolting, Phys. Rev. B **61**, 1386 (2000).
[16] I.A. Nekrasov, K. Held, N. Blümer, A.I. Poteryaev, V.I. Anisimov, and D. Vollhardt, Eur. Phys. J. B **18**, 55 (2000).
[17] R. M. Dreziper and E. K. U. Gross, in *Density Functional Theory* (Ref. 2), Chap. 7.
[18] J.P. Perdew, K. Burke, and M. Ernzerhof, Phys. Rev. Lett. **77**, 3865 (1996).
[19] O. Gunnarsson and R.O. Jones, Phys. Scr. **21**, 394 (1980).
[20] R.T. Sharp and G.K. Horton, Phys. Rev. **90**, 317 (1953).
[21] J.D. Talman and W.F. Shadwick, Phys. Rev. A **14**, 36 (1976).
[22] M. Stadele, J.A. Majewski, P. Vogl, and A. Gorling, Phys. Rev. Lett. **79**, 2089 (1997).
[23] T. Kotani and H. Akai, Physica B **237–238**, 332 (1997).
[24] L. Hedin and B.I. Lundquist, *Solid State Physics*, edited by F. Seitz, D. Turnbull, and H. Ehrenreich (Academic Press, New York, 1969), Vol. 23, p. 1.
[25] For a recent review see: W. Aulbur, L. Jönsson, and J. W. Wilkins in *Solid State Physics*, edited by H. Ehrenreich and F. Spaepa (Academic Press, New York, 2000), Vol. 54, p. 2.
[26] N. Marzari and D. Vanderbilt, Phys. Rev. B **56**, 12 847 (1997).
[27] O.K. Andersen, Phys. Rev. B **12**, 3060 (1975).
[28] H. L. Skriver, *The LMTO Method* (Springer-Verlag, Heidelberg 1984).
[29] V.L. Moruzzi, J.F. Janak, and A.R. Williams, *Calculated Electronic Properties of Metals* (Pergamon, New York, 1978).
[30] I. Schnell, Thesis, University of Bremen, 2002, available at: www-theorie.physik.uni-bremen.de/ischnell/thesis
[31] G. Stollhoff, Phys. Rev. B **58**, 9826 (1998).
[32] G.D. Mahan, *Many-Particle Physics* (Plenum Press, New York, 1990).
[33] C. Pisani and R. Dovesi, C. Roetti, *Hartree-Fock Ab Initio Treatment of Crystalline Systems*, Lecture Notes in Chemistry, Vol. 48 (Springer-Verlag, Berlin, 1988); C. Pisani, *Quantum-Mechanical Ab-initio Calculation of the Properties of Crystalline Materials*, Lecture Notes in Chemistry, Vol. 67 (Spinger Verlag, Heidelberg, 1996).
[34] H.J. Monkhorst, Phys. Rev. B **20**, 1504 (1979).
[35] R. Dovesi, C. Pisani, F. Ricca, and C. Roetti, Phys. Rev. B **25**, 3731 (1982).
[36] V. Sahni, J. Gruenebaum, and J.P. Perdew, Phys. Rev. B **26**, 4371 (1982).
[37] D.M. Bylander and L. Kleinman, Phys. Rev. Lett. **74**, 3660 (1995); Phys. Rev. B **52**, 14 566 (1995).
[38] T. Kotani, Phys. Rev. B **50**, 14 816 (1994).
[39] T. Kotani, Phys. Rev. Lett. **74**, 2989 (1995).
[40] I. Schnell, G. Czycholl, and R.C. Albers, Phys. Rev. B **65**, 075103 (2002).
[41] J.C. Slater, Phys. Rev. **34**, 1293 (1929).
[42] R.E. Watson, Phys. Rev. **118**, 1036 (1959); **119**, 1934 (1959).
[43] L. Hodges, R.E. Watson, and H. Ehrenreich, Phys. Rev. B **5**, 3953 (1972).
[44] U. von Barth and L. Hedin, J. Phys. C **5**, 1629 (1972).
[45] T. Kotani and H. Akai, J. Magn. Magn. Mater. **177**, 569 (1998).
[46] For a review see; A. George, G. Kotliar, W. Krauth, and M.J. Rozenberg, Rev. Mod. Phys. **68**, 13 (1996).
[47] W. Weber, J. Bünemann, and F. Gebhard, in *Band-Ferromagnetsim*, edited by K. Baberschke, M. Donath, and W. Nolting, Lecture Notes in Physics, Vol. 580 (Springer, Berlin, 2001), p. 9.; J. Bünemann, W. Weber, and F. Gebhard, Phys. Rev. B **57**, 6896 (1998).